Evidence for a large to very large earthquake around A.D. 1100 on the Himalayan Frontal Thrust

J. Lavé[1*], D. Yule[2*], S. Sapkota[3], K. Basant[3], C. Madden[4], M. Attal[1], and R. Pandey[3]

1- Laboratoire de Géodynamique des Chaînes Alpines, BP53, 38041 Grenoble, France.

2- California State University, Northridge, California, USA.

3- Seismolab, Department of Mines and Geology, Lainchaur, Kathmandu, Nepal.

4- Earth Consultants International, Orange, California, USA.

** These authors contributed equally to the work.*

corresponding author : J. Lavé _ E-mail: jlave@ujf-grenoble.fr

Submitted to: Science

The Himalayan orogen has produced four M_w7.8 to 8.4 thrust earthquakes during past century. Despite their great magnitude, no surface ruptures associated with these earthquakes have been documented. Here, we present paleoseismologic evidence from east-central Nepal that an earthquake ruptured the Main Frontal Thrust fault at ~A.D. 1100, with a surface displacement of ~17 $^{+5}/_{-3}$ m. Based on paleoseismologic results in Far East Nepal (*1*), we hypothesize that the lateral extent of the ~A.D. 1100 earthquake could have exceeded 300 km, and that its size could have reached ~M_w9.0. In this preferred scenario, ruptures associated with M_w<8.5 events would die out upward, with, however, co- and post-seismic deformation substantially contributing to the folding of the most frontal Himalayan structures (*2*). This implies significant modifications to current seismotectonic models based on the historical seismicity and to seismic hazard estimation in this densely populated region.

The Himalaya is the most prominent and active intracontinental range in the world. Though the gross features of this active orogen are now understood. the details of its seismotectonic behavior and maximum magnitudes are mostly unknown, despite their important implications for the seismic hazard facing hundreds of millions of people living in the region. During the past century, the Himalayan arc has experienced four major thrust earthquakes of M_w>7.8. Growth folding (*2, 3*) and surface faulting (*1, 4*) have been reported in Holocene strata and terraces: paradoxically, none of these recent events reportedly

produced coseismic surface ruptures, including the 1934 Bihar Nepal M_w8.4 earthquake. To confirm the absence of rupture associated with this event and determine which events have led to the tectonic scarps, we conducted a paleoseismologic study across the Himalayan front in the Marha Khola region, southeast of Kathmandu, in an area hard hit by the 1934 event.

The Himalaya results from the collision between India and the southern edge of Eurasia. Since ~20 Ma the deformation front resulting from this collision is expressed through the activation of major thrust zones (*5*): the Main central Thrust (MCT) and the Main Boundary Thrust (MBT). These two faults are presumed to branch upward from a major mid-crustal decollement, the Main Himalayan Thrust (MHT) (*6-10*) (Figure 1). In front of the rising Himalaya, thin-skinned thrust-faulting has incorporated Cenozoic molasse deposits (Siwaliks Formations) into the hanging walls of several thrusts also branching from the MHT (*2, 7*), now expressed as the low-relief Siwaliks Hills – or Subhimalaya – at the front of the range. The most frontal of these thrusts, called Main Frontal Thrust fault (MFT), marks the active deformation front (*3*).

In central Nepal, active deformation appears to be concentrated in the Siwaliks Hills: all along the frontal fold, geomorphic evidence for active tectonics indicates that 50 to 100% of the shortening across the Himalayas is transferred toward the frontal thrusts (*2, 4, 11*). However, geodetic measurements (*12-13*) show that strain currently is accumulating at the foot of the High Himalaya (HH), 70 to 100 km north of the MFT. Concomitantly, this strain build-up is accompanied by seismicity (M_w5-7) concentrated at the base of the HH (*14*) (Figure 1). One explanation of this apparent paradox proposes that this deformation mostly

represents interseismic elastic deformation that accumulates on the MHT below the HH and that this deformation releases and transfers to the front during large earthquakes (*2, 9*). In 1934, a M_w8.4 earthquake hit east Nepal, with a lateral extent south of Kathmandu to the eastern Indian border, and high intensity shaking experienced 200 km south of the Himalayan front in the Indian region of Bihar (Figure 1).

The study area at Marha Khola is located north of the maximum intensity felt during this 1934 event, and occurs on the Bagmati/Ratu anticline (*15*) where numerous folded fluvial Holocene terraces indicate a full transfer of the convergence to the frontal structure (*2*). Along the Mahra Khola, Holocene fluvial strath terraces (HT0 to HT5 in Figure 2) have been uplifted 5 to 40 m above its present channel. A tectonic scarp marks the southern extent of these terraces (*15*). The scarp is ~4 m high across the youngest uplifted terrace (HT4) and exhibits a relatively sinuous geometry, with two east-west segments connected by a north-south segment (Figure 2).

Two trenches were excavated across this scarp (Trenches T1 and T2) and one river bank exposure (T3) was cleaned and extended to depth by a small trench excavation (Figure 2). These three exposures show similar relationships regarding the size and timing of the surface rupture at the scarp (Figures 3 and 4a). Upper Siwaliks siltstone to fine conglomerate exposed in the lowest strath terrace show zones of clay gouge at the fault and elsewhere in the hanging wall. Above the strath, the thickness of the fluvial sequence (unit 1, Figures 3 and 4a) is relatively uniform at ~3 m (Figure 4). The fluvial material above the strath was deposited around A.D. 700 (Figure 4b and (*15*), samples MA-4 and M-2-29). On top of this sequence a 20-cm-thick, organic-rich soil has developed within (in T3) or right

above overbank deposits (in T2): charcoal samples in the paleosol yield calibrated ages of A.D. 1000 to 1200 (samples M-3-5 and M-2-9). At T1, small stream incised into terrace HT3 (Figure 2) deposited >2.5 m of fine to coarse fan material, with interlayered thin soil horizons, on the footwall from A.D. 700 to at least A.D. 950 (samples M-1-46,53 and M-1-31). The thick soil at T2/T3 and interlayered fan deposits/thin soils at T1 are considered unit 2 lateral equivalents. Fluvial incision has truncated units 1 and 2 along a major unconformity, $U_{2\text{-}3}$. In T2, the unconformity is immediately overlain in its western part by a sequence of fluvial gravels (unit 3) that bury the footwall and deposit a thin veneer on top of the frontal fold (Figure 3). Charcoal from unit 3 provides calibrated ages of A.D. 1000 to 1200 (samples M-2-6, 25, and 22), and was deposited probably soon after unit 2 deposition and $U_{2\text{-}3}$ beveling. Subsequently, in all trenches, sequences of weak soil, slope wash, overbank and fluvial materials (unit 4) were deposited from A.D. 1000 to 1900 (samples M-3-4, M-2-7, 12, 27 and M-1-61, 26, 24), culminating with the present-day 40-cm-thick cultivated soil (Figure 3).

The tectonic scarp is the combined result of faulting and folding. In each trench, three rupture zones (F1, F2 and F3), comprised of three to six faults, have ruptured the fluvial sequence (units 1 and 2) and are sealed by units 3 and 4. The vertical separation of the top of the fluvial sequence between foot- and hanging walls is ~7.5 m (Figure 4). The frontal ruptures (F3) are associated with important folding and have clearly recorded an earthquake at about A.D. 1100 (Figure 4b). For the upper ruptures F1 and F2, because they are in the hanging wall of F3, intermediate units and erosion make it more difficult to constrain the timing of their rupture, but a careful analysis of ruptures relationships in T2 indicates that

F1 is most probably coeval of F3 (*15*). In T1, the ruptures F2 and F1 override unit 2 and are sealed by unit 4. They are thus younger than ~A.D. 900 and older than ~A.D. 1150.

To explain the rupture chronology, we could imagine a complex scenario with multiple erosional unconformity-forming episodes and two large ruptures spanning <200 years, or <400 years if the samples from units 3 and 4, that yield AD 1000-1250 calendar ages, are reworked from the youngest part of unit 2 (*15*). However, the simplest explanation of our stratigraphic and structural observations, the existence of one major unconformity that post-dates the ruptures along the MFT and the straightforward interpretation of radiocarbon ages, is to conclude that all the ruptures are coeval and associated with a mega-rupture ~A.D. 1100 (Figure 4).

The amount of slip in the different trenches can hardly be computed by measuring offset in sedimentary layers. However, assuming that the fluvial sequence was initially almost uniform and 3 m thick (Figure 4), slip values can be estimated from the vertical separation, at some distance from the fault, of either the top of the fluvial sequence (unit 1) or the strath level, and from the apparent dip of the fault segment. The three trenches, as the 7-7.5m vertical separation of HT_4 produced by seismic slip on an ~25° dipping ramp (*15*), provide consistent slip estimates of 17 +5/-3m (Table 1) (*16*). The frontal ruptures F3 account for ~25%, ~40% and ~55% of the total slip in T1, T2 and T3 respectively: such lateral variations in slip partitioning are thus fairly consistent with a single mega-rupture scenario.

According to the classical view on scaling between slip value, rupture area, and magnitude, we could first expect that the ~A.D. 1100 earthquake ruptured a large segment of the Himalayan arc. Interestingly, a trench across the MFT in the far East Nepal (*1*)

exposed a rupture with 4 to 8 m of slip that occurred between A.D. 1050 to 1300 (Figure 4b): therefore this surface rupture could also result from the ~A.D. 1100 earthquake. If so, the lateral extent of the rupture exceeds 300 km, a length that has been ascribed to the 1934 M_w8.4 earthquake (*17*) (Figure 1). Assuming that the slip observed in the Marha Khola trench is representative of the average slip on the fault plane, the MHT could have generated a M_w close to 9.0 (*18*), like the 1964 Alaskan and 1960 south-central Chile megathrust earthquakes. According to magnitude distribution law for thrusts earthquakes of central Nepal (*19*) the return period for a ~M_w9.0 event would range between 1000 and 1500 years. Very large earthquakes like the ~A.D. 1100 event would thus accommodate 50 to 75% of the shortening across the Himalaya.

One of the major conclusions of this study is the absence of surface rupture during the M_w8.4 1934 Bihar Nepal earthquake, confirming previous reports (*18*). The rupture could have broken the vertical northern branch of the fault propagation fold (*15*) but we did not observe tectonic scarp across this northern fault. The surface ruptures could have broken a small segment of the MFT directly south of the epicenter, but it would be in some way contradictory with the maximum shaking intensity felt just southeast of Marha Khola (Figure 1). Finally, leveling measurements that show subsidence in the Gangetic plain (*20*) contradict the hypothesis of a rupture propagating south of the MFT (*6*). We thus suspect that the 1934 rupture died out before reaching the surface, but stopped close enough to the surface to transfer most of the slip to the frontal fold as observed in the Bagmati-Bakeya area (*2*). We hypothesize that the upper 2 km of unconsolidated upper Siwaliks units therefore represent a zone of velocity strengthening through which only very large

earthquakes can break. According to this hypothesis, in the shallow reaches of the fault zone, the rupture associated with large M_w<8.5 events would decelerate before reaching the surface and would not create surface ruptures. However, co-seismic and post-seismic deformation would substantially contribute to the long-term folding of the most frontal Himalayan structures.

As an alternative to the megathrust scenario, we can not exclude that the ~1100 A.D. earthquake produced a local high slip value at Marha Khola that is distinct from the event recorded in Far East Nepal and, like the M_w7.6 Chi-Chi earthquake (*21-22*), is associated with the activation of a relatively small portion of the seismogenic decollement and to a M_w between 7.5 and 8. Such an earthquake would release elastic strain accumulated below the LH or the Siwaliks, at the southern extent of ruptures nucleated at the locking transition below the HH. Present GPS measurements along the Himalayan arc in Nepal show slip locking below the HH, and suggest minimal tectonic loading occurs on the southern portion of the MHT. Such a scenario would thus imply limited or no strain recovery under high stress during the past thousand years, but does not explain, however, why none of the major Himalayan earthquakes of the past century has produced surface ruptures.

In any case, if evidence of M_w<8.5 earthquakes, like the 1934 earthquake, is difficult to observe at the surface, this would have major implications on the way paleoseismologists and engineers could assess seismic hazard and earthquakes recurrence from superficial trenches in such settings. Historical accounts report two $7 \leq M_w \leq 8$ in east Nepal in 1833 and 1866 (*23-24*). Strong earthquakes partly destroyed Kathmandu in 1255 and 1344 (*25*), but they can be ascribed to a MHT segment farther west or to shallower faults close to the

Kathmandu basin. None of these earthquakes have been observed in the Marha Khola trenches, and we suspect that, per thousand year period, the MHT can generate one ~M_w9.0 megathrust earthquake and several 7.5<M_w<8.5 major events. In view of the disastrous consequences to the many tens of millions of inhabitants of northern India and Nepal, it thus becomes urgent to pursue additional paleoseismologic work in this region.

References and notes

1. B.N. Upreti, et al., Eds. (*Proc. of the Hokudan Intern. Symposium and School on Active Faulting*, pp. 533-536 (Letter Press Ltd., Hiroshima, Japan, 2000).

2. J. Lavé, J.P. Avouac, *J. Geophys. Res.* **105**, 5735 (2000).

3. T. Nakata, *Spec. Pap. Geol. Soc. Am.* **232**, 243 (1989).

4. S. Kumar et al., *Science* **294**, 2328 (2001).

5. A. Gansser, *Geology of the Himalayas* (Inter-Science Publisher, 1964).

6. L. Seeber, J. Armbuster, Eds., *Earthquake Prediction : An International Review*, pp. 259-277 (Maurice Ewing Series, Am. Geophys. Un., Washington D. C., 1981).

7. D. Schelling, K. Arita, *Tectonics* **10**, 851 (1991).

8. W. Zhao, K.D. Nelson, project INDEPTH Team, *Nature* **366**, 557 (1993).

9. M.R. Pandey, R.P. Tandukar, J.P. Avouac, J. Lavé, J.P. Massot, *Geophys. Res. Let.* **22**, 751 (1995).

10. J. Lavé, J.P. Avouac, *J. Geophys. Res.* **106**, 26,561 (2001).

11. S.G. Wesnousky, S. Kumar, R. Mohindra, V.C. Thakur, *Tectonics* **18**, 967 (1999).

12. M. Jackson, R. Bilham, *J. Geophys. Res.* **99**, 13897 (1994).

13. R. Bilham, K. Larson, J. Freymuller, Project Idylhim members, *Nature* **386**, 61 (1997).

14. J. Ni, M. Barazangi, *J. Geophys. Res.* **89**, 1147 (1984).

15. Supplementary material is available at www.sciencemag.org/...

16. We assume that the surface rupture at Marha Khola area had a slip direction close to the N198 Himalayan shortening direction (*2*) (Figure1), and therefore that the ruptures likely have a strike-slip component on the fault planes. Two methods for geometric correction have been considered. (Method A) No re-orientation of the slip occurs close to the surface perpendicular to the scarp. In that case, the slip value Δl on a fault dipping at an angle θ and with a strike making an angle $\Delta\varphi$ with the mean Himalayan slip vector can be computed from the vertical offset Δh recorded by a marker following: $\Delta l = \Delta h / \sin(\arctan(\sin(\Delta\varphi).\tan(\theta)))$. (B) Slip partitioning occurs between strike-slip motion on the pop-up structure (F2) and pure thrust motion on the most frontal, shallow-dipping thrust faults (F3). In that case, we assume that thrust motion on the frontal faults is perpendicular to the tectonic scarp, i.e. in our case parallel to the trench axis. Slip value writes simply as $\Delta l = \Delta h / \sin(\theta)$. Taking into account the slip obliquity (Method A), except on the frontal rupture F3 in T2 (Method B), leads to relatively consistent results between the different trenches (Table 1).

17. M.R. Pandey, P. Molnar, *J. Geol. Soc. Nepal* **5**, 22 (1988).

18. Moment magnitude was computed from Kanamori's relation [H. Kanamori, *Tectonophysics* **93**, 185 (1983)] for the seismic moment $Mw=2/3\log_{10}(M_0)$ - 6 where $M_0=\mu*slip*L*W$, the shear modulus $\mu=3.3\text{x}10^{10}$ N/m^2, W=100 km from the locking zone below the HH to the MFT, L≥300km and average slip equal to 17 m. Recent theoretical modeling [D.D. Oglesby, R.J. Archuletta, S.B. Nielsen, *Bull. Seism. Soc. Am.* **90**, 616 (2000)] and observations during Chi-Chi earthquake would suggest that dip-slip amplification could occur close to the surface for thrust faults. If it has been the case for the MFT in Marha Khola, the 17 m slip would represent a maximum value.

19. J.P. Avouac, L. Bollinger, J. Lavé, R. Cattin, M. Flouzat, *C. R. Acad. Sc.* **333**, 513 (2001).

20. R. Bilham, F. Blume, R. Bendick, V. Gaur, *Current Science* **74**, 213 (1998).

21. H.F. Ma, *Eos Trans. AGU* **80**, 605 (1999).

22. S. Dominguez, J.P. Avouac, R. Michel, *J. Geophys. Res*. **108**, 2083, doi: 10.1029/2001JB000951 (2003).

23. R.D. Oldham, *Memoir of the Geol. Surv. of India* **19**, 163 (1883).

24. R. Bilham, *Current Science* **69**, 101 (1995).

25. M.R. Pant, *Adarsa* **2**, 29 (2002).

26. J. Suppe, *Amer. Jour. Sci.* **283**, 684 (1983).

27. K. Larson, R. Bürgmann, R. Bilham, J. Freymueller, *J. Geophys. Res.* **104**, 1077 (1999).

28. P. Molnar, *J. of Him. Geol.* **1**, 131 (1990).

29. W.P. Chen, P. Molnar, *J. Geophys. Res*. **82**, 2945 (1977).

30. R. Chander, *Tectonophysics* **170**, 115 (1989).

31. M. Stuiver, P.J. Reimer, *Radiocarbon* **35**, 215 (1993).

32. This research was supported by the French program PNRN. We are most grateful to the National Seismological Center (DMG, Kathmandu) and Laboratoire de Détection Géophysique (LDG) for their logistic help in the organization of the field surveys. A. Gajurel kindly provided help logging the trenches. We are indebted to Dr. G. Seitz for analyzing some of the charcoal samples at the Center for Accelerator Mass Spectrometry, Lawrence Livermore National Laboratory, California, USA. We thank J.P. Avouac and K. Sieh for insightful comments on an early draft of the manuscript.

Table 1: Vertical Offsets, Fault Orientations, and Slip Calculations

	ruptures	vertical offset[§] (m)	fault strike relative to N198 (°)	fault dip (°)	Slip value (m) with oblique slip
Trench 1	F3	1.1 ± 0.3	50 ± 10	20 ± 5	4.1 $^{+4.2}_{-2.0}$
	F2	3.7 ± 0.5	30 ± 5	43 ± 3	8.8 $^{+3.8}_{-2.5}$
	F1	1.5 ± 0.3	30 ± 5	43 ± 4	3.5 $^{+2.0}_{-1.3}$
	Total	6.3 ± 0.3			16.4 $^{+7.8}_{-3.5}$
Trench 2	F3	3.2 ± 0.3	25 ± 5	[‡]17, 30 ± 4	13.5 $^{+1.6}_{-1.2}$ [#]6.4
	F1	4.0 ± 0.3	25 ± 5	44 ± 2	10.6 $^{+4.0}_{-2.5}$
	Total	7.2 ± 0.3			24.1 $^{+4.8}_{-3.0}$ [#]17.0
Natural exposure	F3	5.1 ± 0.5	55 ± 10	[‡]20, 38 ± 4	9.5 $^{+4.6}_{-2.7}$
	F2	1.1 ± 0.2	55 ± 10	18 ± 2	[†]3.9 $^{+2.3}_{-1.4}$
	F1	1.9 ± 0.2	55 ± 10	36 ± 7	[†]3.5 $^{+2.0}_{-1.1}$
	Total	8.1 ± 0.3			16.9 $^{+6.7}_{-3.1}$
HT_4 uplift		7.2 ± 0.6	90	*25 ± 5	17.0 $^{+5.8}_{-3.8}$

([§])Vertical offset calculated based on the offset of the HT_4 strath or terrace top assuming a fluvial sequence 3 m thick above the strath.

([†]) Slip computed from line restoration technique applied to the strath level.

([‡]) For the frontal ruptures, the important folding observed in the hanging wall can be explained by fault-steepening at depth: the first dip value corresponds to superficial fault dip in the trench, whereas the second value corresponds to the dip at depth, which has been estimated by applying fault-bend-fold geometric rules (*26*) and has been used for subsequent calculations.

([#]) Slip computed assuming strike-slip partitioning on the pop-up structure F2 and pure thrusting on F3 ruptures.

(*) Fault dip estimate according to fold cross-section (*15*).

Figure Legends

Figure 1: (a) Topographic and seismotectonic map of central and eastern Nepal, including GPS velocities relative to GPS stations in Gangetic Plain (*2, 27*), and the focal mechanisms of the major earthquakes (M_w>5) since 1965 [ISC; Harvard solution; (*28*)] that indicate a present Himalayan shortening direction close to N190-200. The major faults are the Main Central Thrust (MCT), the Main Boundary Thrust (MBT), and the Main Frontal Thrust (MFT). In 1934, this region of Nepal experienced a large earthquake (epicenter shown by red star) (*29*), which has been attributed to the Himalayan thrust structures but which has mostly shaken the Gangetic plain to the south of the MFT, as evidenced by the isoseismal zones (red lines) (*30*). The Marha Khola trench site (A) is located in the western part of the most heavily shaken area, at the opposite end of the zone of strong shaking from a previous paleoseismologic trenching study (C) in Far East Nepal (*1*). Across the Bagmati river (B), 30 km west of Marha Khola, the MFT has been recognized to slip at a rate of 21±1.5 mm/yr during the Holocene (*2*). (b) Simplified structural cross-section across the central Himalaya of Nepal with the major instrumental thrust earthquakes since 1965 (red circles) and the cluster of microseismicity (*9*) (purple shading).

Figure 2: Topographic map of the trench site showing the MFT tectonic scarp and faulted terraces on the right bank of Marha Khola with the two trenching sites (T1 and T2) across the scarp and the enhanced river bank exposure (T3).

Figure 3: Log of the NW wall of trench 2. Triangles show locations of charcoal samples, with AMS radiocarbon dating maximum age ranges. All dates (2σ) have been calibrated using the CALIB 4.3 program (*31*). All dates are in calendar years A.D., unless otherwise noted.

Figure 4: (a) Schematic view of the topographic survey of HT4 terrace and fault scarp along the right bank of Marha Khola and of the 3 trenches with the major units and faults (logs are projected on the mean axis of each trench). Elevations are given relative to the elevation of the present river. Sample numbers are abbreviated to their last identifying number (for example, number 7 in trench 2 correspond to the sample M-2-7). Note that the strath level is nearly uniform between the exposed bank and the trenches, and that the fluvial sequence above the strath is also uniformly 3 m thick. (b) Summary of the dating results in stratigraphic order of Marha Khola's trenches (*15*) and from a trench in far East Nepal (*1*).

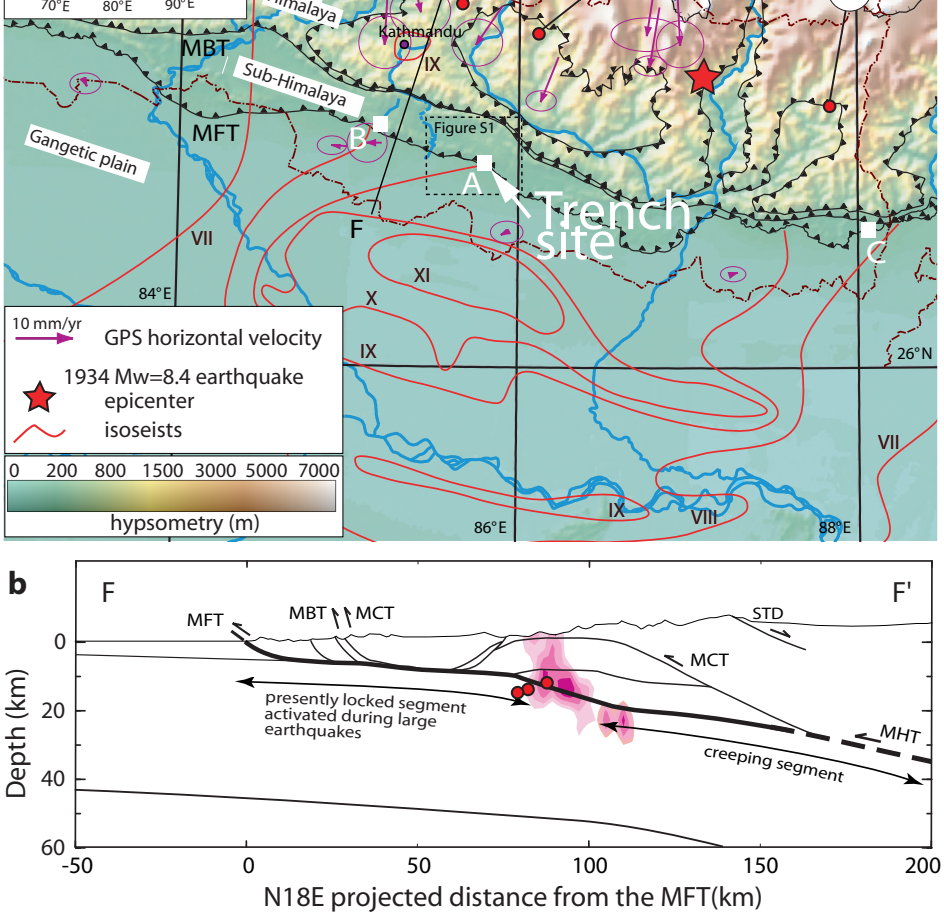

Figure 1

(125% larger than the estimated final size)

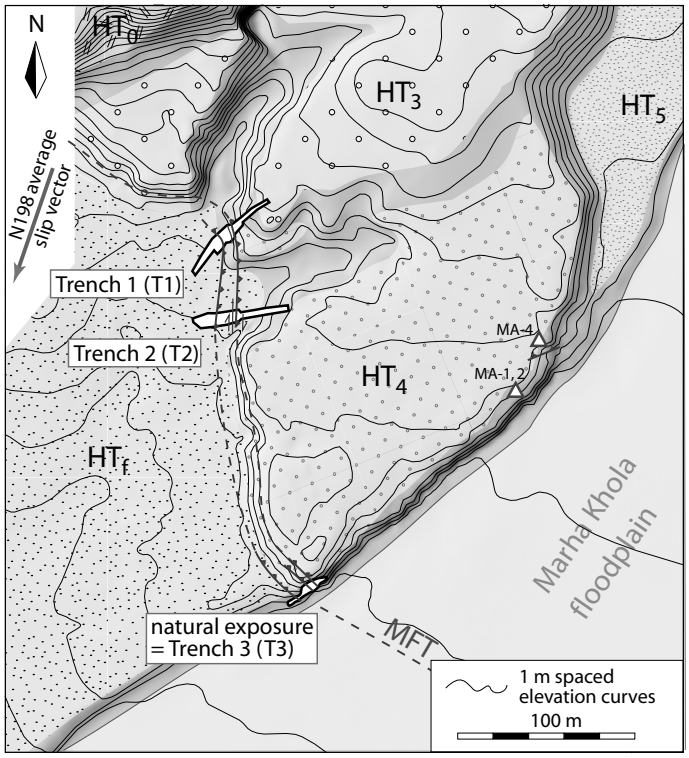

Figure 2

(150% larger than the estimated final size)

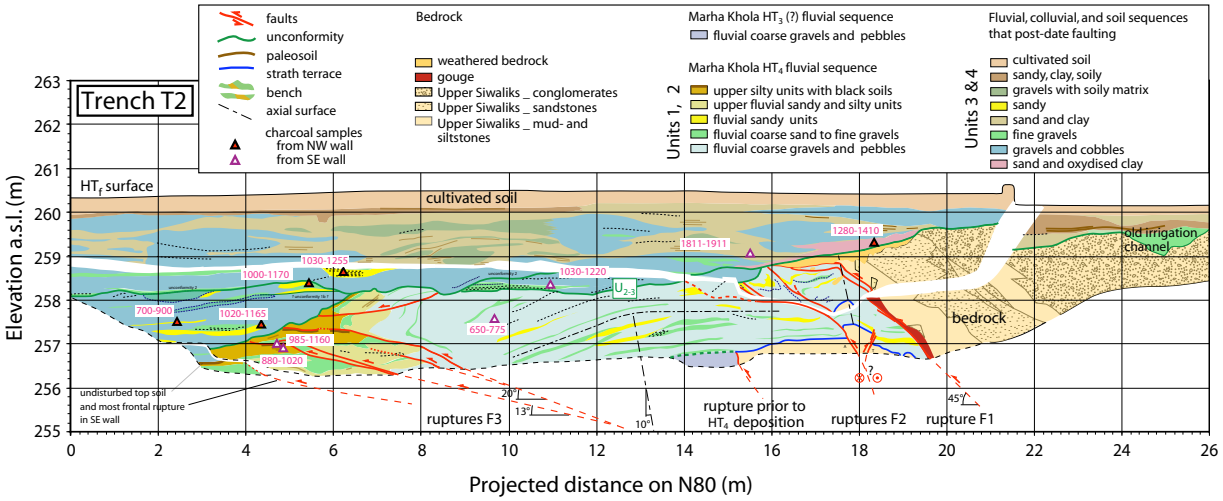
Trench T2
faults
unconformity
paleosoil
strath terrace
bench
axial surface
charcoal samples
from NW wall
from SE wall
Bedrock
weathered bedrock
gouge
Upper Siwaliks _ conglomerates
Upper Siwaliks _ sandstones
Upper Siwaliks _ mud- and siltstones
Marha Khola HT3 (?) fluvial sequence
fluvial coarse gravels and pebbles
Marha Khola HT4 fluvial sequence
upper silty units with black soils
upper fluvial sandy and silty units
fluvial sandy units
fluvial coarse sand to fine gravels
fluvial coarse gravels and pebbles
Units 1, 2
Fluvial, colluvial, and soil sequences that post-date faulting
cultivated soil
sandy, clay, soily
gravels with soily matrix
sandy
sand and clay
fine gravels
gravels and cobbles
sand and oxydised clay
Units 3 &4
HTf surface
cultivated soil
old irrigation channel
bedrock
1280-1410
1811-1911
1030-1255
1000-1170
1030-1220
700-900
1020-1165
650-775
985-1160
880-1020
U2-3
undisturbed top soil and most frontal rupture in SE wall
ruptures F3
rupture prior to HT4 deposition
ruptures F2
rupture F1
20°
13°
10°
45°
Elevation a.s.l. (m)
Projected distance on N80 (m)

Figure 3

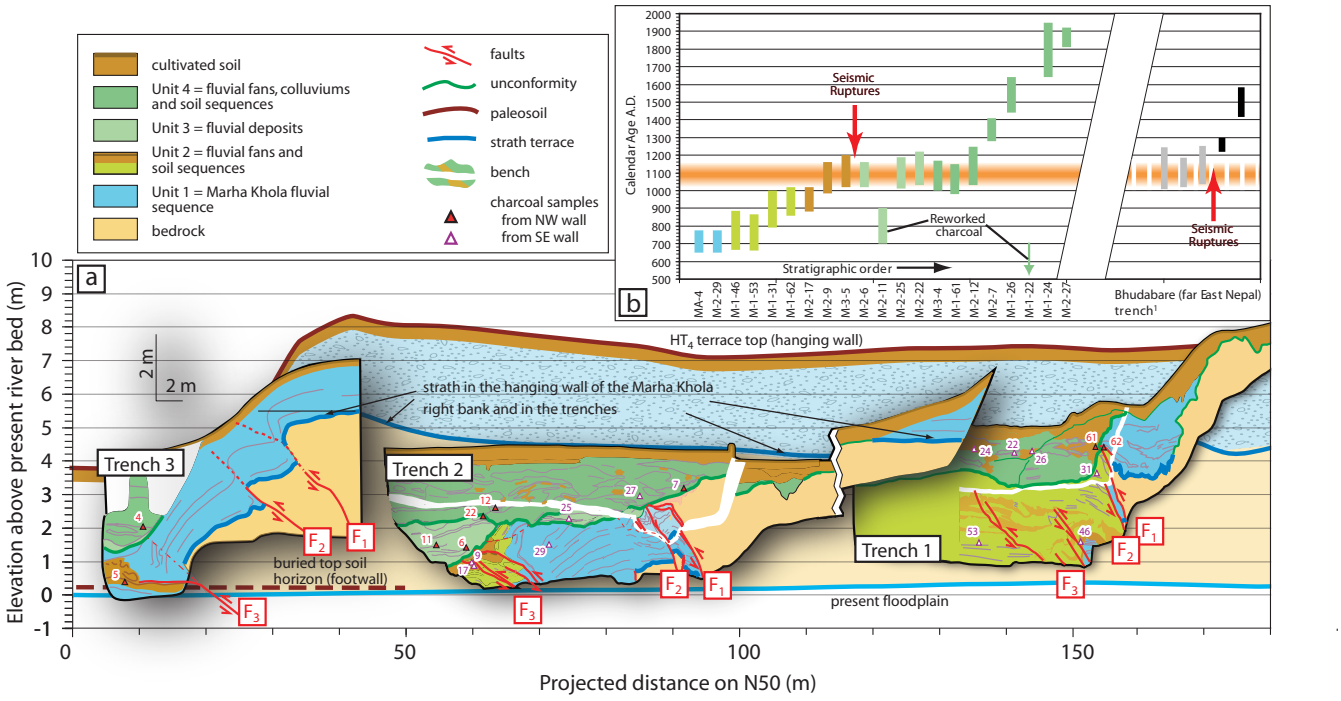
cultivated soil
Unit 4 = fluvial fans, colluviums and soil sequences
Unit 3 = fluvial deposits
Unit 2 = fluvial fans and soil sequences
Unit 1 = Marha Khola fluvial sequence
bedrock
faults
unconformity
paleosoil
strath terrace
bench
charcoal samples from NW wall
from SE wall
a
b
Calendar Age A.D.
Seismic Ruptures
Reworked charcoal
Stratigraphic order
Bhudabare (far East Nepal) trench1
HT4 terrace top (hanging wall)
strath in the hanging wall of the Marha Khola right bank and in the trenches
2 m
Trench 3
Trench 2
Trench 1
buried top soil horizon (footwall)
present floodplain
Elevation above present river bed (m)
Projected distance on N50 (m)

Figure 4

Supplementary information:

Supplementary Discussion: Detailed ruptures relationship in T2

In T2, the F1 rupture is sealed by the unit 4 and is older than ~A.D. 1400 (M-2-7) and probably older than ~A.D. 1200 (M-2-12) if the unconformity between units 3 and 4 has been correctly mapped. The kink in the upper part of the F1 rupture and the overlying bedrock may record a more recent earthquake resulting from the bending of the hanging wall as the fault ruptured onto a paleosurface, i.e. the erosive surface that corresponds to the present major unconformity $U_{2\text{-}3}$. However, this hypothesis is hardly sustainable because there is no soil or weathering on this presumed paleosurface, and because the common feature displayed by faults breaking the surface (F3 in T2 and T3) does not show such sharp bending but shows a continuity of the rupture dip and space accommodation by folded and overturned gravels of the fluvial sequence overlying the bedrock (Figures 3 and 4). These observations added to the dating constraints suggest that F1 rupture is older than the major unconformity $U_{2\text{-}3}$. In a second hypothesis, the kink in F1 geometry would result from folding by the pop-up structure F2 in its footwall. Axial surfaces in the gravels of unit 1 above F2 and F1 kink closely match (Figure 3), and degree of rotation are compatible (~30° and 20-45°, respectively). This scenario would imply that F1 predates or is coeval with F2 and F3. The nature of F2 is not clear for us, but we indeed suspect that this pop-up structure is intimately linked to the frontal rupture F3: either it represents some strike-slip feature that accommodated slip partitioning on this strongly oblique N-S segment of the MFT (the thrust motion being accommodated by F3), or the folding above F3 results from slip reduction toward

the surface and F2 expresses the compressive strain at the fold axis associated with this slip reduction.

Supplementary Table: AMS Radiocarbon (^{14}C) Dates from detrital charcoal collected from Mahra Khola Trenches (T1, T2, and T3) and from HT4 Terrace Exposures.

Unit[#]	Sample Number*	Lab[†]	Measured Radiocarbon Age[‡] (years B.P.)	$\delta^{13}C$ Value[§]	Calibrated Age(s)[@] (calendric, 2σ)
		Trenches			
4	M-2-27	CAMS	75 +/-30	(-25.0)	A.D. 1810 to 1920
4	M-1-24	Beta (177947)	210 +/-40	-24.6	A.D. 1640 to 1690 A.D. 1730 to 1810 A.D. 1920 to 1950
4	*M-1-22*	*Beta (177946 *)*	*2350 +/-40*	*-27.9*	*430 to 380 B.C.* *500 to 460 B.C.*
4	M-1-26	CAMS (‡)	380 +/-50	(-25.0)	A.D. 1440 to 1640
4	M-2-7	Beta (177948 *)	640 +/-40	-26.4	A.D. 1280 to 1410
4	M-2-12	Beta (176837 *)	880 +/-40	-25.4	A.D. 1030 to 1250
4	M-1-61	Beta (176833 *)	1000 +/-40	-25.1	A.D. 980 to 1060 A.D. 1080 to 1150
4	M-3-4	Beta (176840*)	940 +/-40	-28.4	A.D. 1010 to 1190
3	M-2-22	Beta (176839 *)	970 +/-40	-26.9	A.D. 1000 to 1170
3	M-2-25	CAMS (‡)	900 +/-40	(-25.0)	A.D. 1030 to 1220
3	*M-2-11*	*Beta (176836 *)*	*1210 +/-40*	*-28.1*	*A.D. 700 to 900*
3	M-2-6	CAMS (‡)	955 +/-40	(-25.0)	A.D. 1020 to 1160
2	M-3-5	Beta (176841 *)	930 +/-40	-25.0	A.D. 1020 to 1200
2	M-2-9	CAMS (‡)	985 +/-40	(-25.0)	A.D. 985 to 1160

2	M-2-17	Beta (176838 *)	1090 +/-40	-18.5	A.D. 880 to 1020
2	M-1-62	Beta (176834 *)	1130 +/-40	-26.6	A.D. 790 to 1000
2	M-1-31	CAMS (‡)	1105 +/-40	(-25.0)	A.D. 860 to 1020
2	M-1-53	CAMS (‡)	1280 +/-40	(-25.0)	A.D. 660 to 865
2	M-1-46	CAMS (‡)	1260 +/-40	(-25.0)	A.D. 665 to 685
1	M-2-29	CAMS (‡)	1325 +/-40	(-25.0)	A.D. 650 to 775
		Terraces			
HT4	*MA-1*	*CDR (1805 #)*	*6650 +/-60*	*(-25.0)*	*5660 to 5480 B.C.*
HT4	*MA-2*	*CDR (1753 #)*	*3970 +/-65*	*-25*	*2660 to 2290 B.C.*
HT4	MA-4	CDR (1754 #)	1310 +/-40	-26.22	A.D. 655 to 780

Italics denote those samples that we interpret as having been reworked.

[#]See trench logs for stratigraphic unit designations

*Trench number indicated by second number in sequence, e.g., sample M-2-27 was collected from T2.

[†]Beta, Beta Analytic, Inc., Miami, FL, USA; CAMS, Center for Accelerator Mass Spectrometry, Lawrence Livermore National Laboratory, Livermore, CA, USA; CDR, Centre de datation par le radiocarbone, Université C. Bernard Lyon 1, France. Lab numbers in parentheses.

[‡]Radiocarbon years B.P. relative to 1950 (with 1s counting error).

[§]Parentheses denote samples for which $\delta^{13}C$ values are unavailable and assumed to be -25.0 ‰.

[@]Calendric dates were calibrated using MacCALIB 4.3 (*31*), using their calculation method B. In accordance with their recommendations, calendric ages have been rounded to the nearest ½ decade and decade for samples with standard deviation in the radiocarbon ages less than and greater than 50 years, respectively.

Supplementary Figure S1: (a) Geological map of the Siwaliks fold in the Bagmati-Marha-Ratu area. Despite the presence of numerous uplifted Holocene terraces along most of the rivers, the fault scarps associated to the MFT (thick purple line) are restricted to the lowest elevation area of the frontal fold between Marha Khola and Aurhi Khola (western river in the figure). (b) Cross section at Marha Khola showing the small frontal splay of the MFT, distinctive from most of the Bagmati-Ratu anticline, with the existence of a 2-km-wide slice of Plio-Pleistocene upper Siwaliks units at the front of the range and probably resulting from fault propagation folding stepping to the south of the main trace of the MFT. MDT = Main Dun Thrust.

Supplementary Figure S2: Photo-mosaic of the cleaned natural exposure showing three faults (F1/F2/F3, right/middle/left, respectively) and folding associated with surface deformation on the MFT, right bank of Mahra Khola.

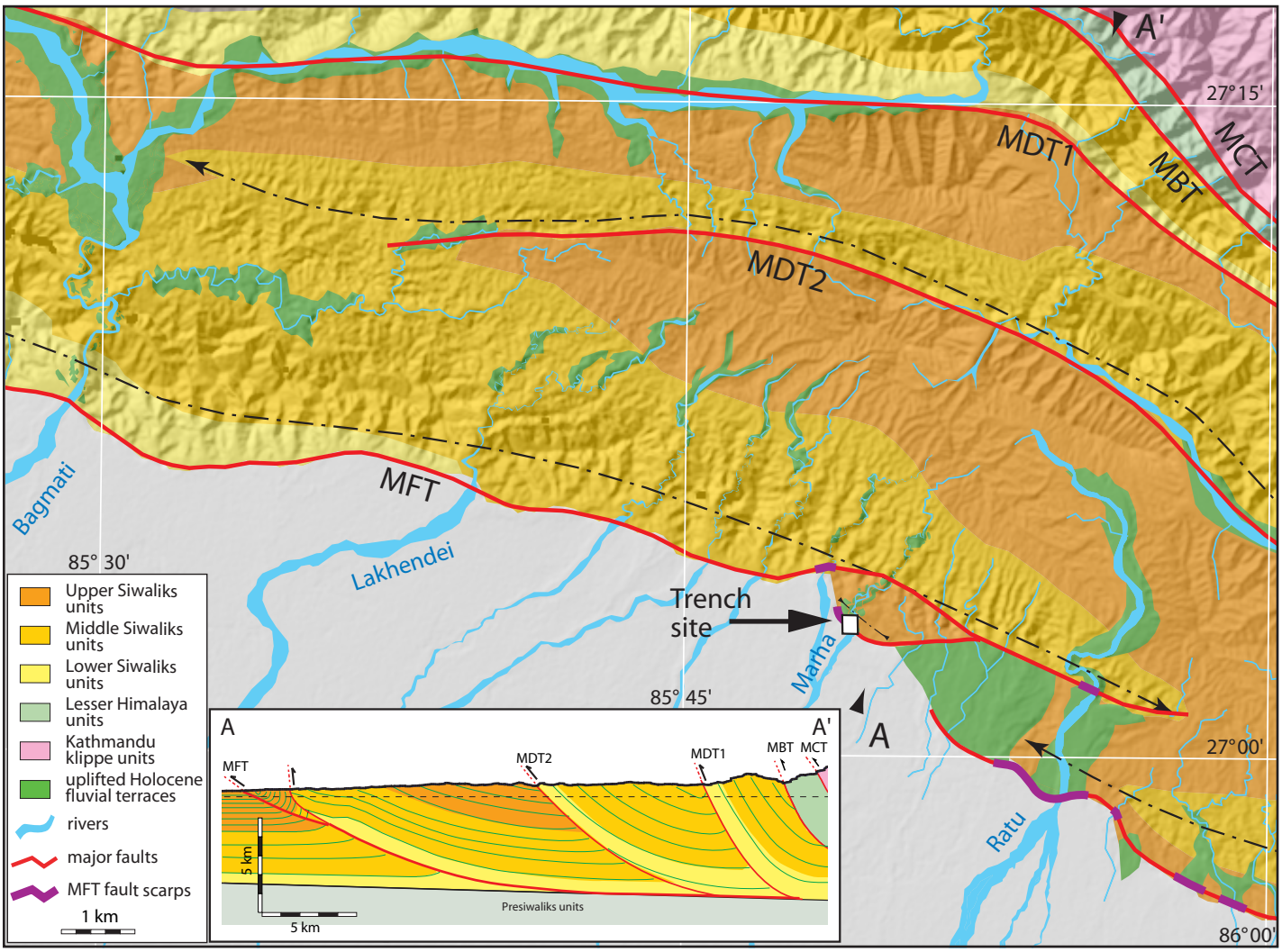

Supplementary Figure S1

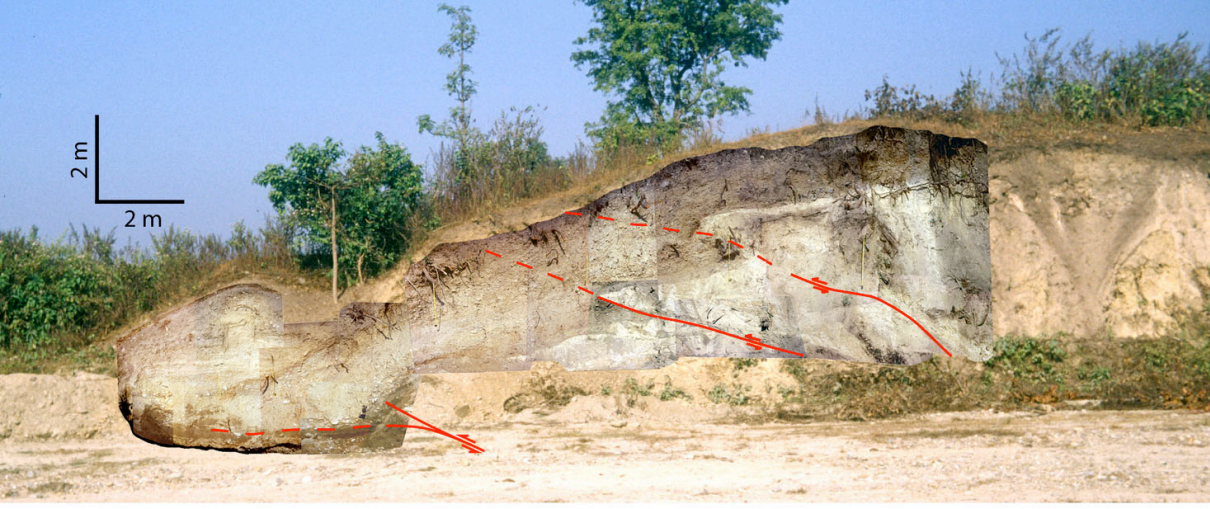

Figure S2